Published in Computer Methods in Biomechanics and Biomedical Engineering, 18(5): pp. 477-484. DOI: 10.1080/10255842.2013.818662

On modelling large deformations of heterogeneous biological tissues using a mixed finite element formulation

This paper addresses the issue of modelling material heterogeneity of incompressible bodies. It is seen that when using a mixed (displacement-pressure) finite element formulation, the basis functions used for pressure field may not be able to capture the nonlinearity of material parameters, resulting in pseudo residual stresses. This problem can be resolved by modifying the constitutive relation using Flory's decomposition of the deformation gradient. A two-parameter Mooney-Rivlin constitutive relation is used to demonstrate the methodology. It is shown that for incompressible materials, the modification does not alter the mechanical behaviour described by the original constitutive model. In fact, the modified constitutive equation shows a better predictability when compared against analytical solutions. Two strategies of describing the material variation (i.e. linear and step change) are explained and their solutions are evaluated for an ideal two-material-interfacing problem. When compared with the standard tied coupling approach, the step change method exhibited a much better agreement due to its ability to capture abrupt changes of the material properties. The modified equation in conjunction with integration points based material heterogeneity is then used to simulate the deformations of heterogeneous biological structures to illustrate its applications.

Keywords: heterogeneous material; hyperelastic constitutive relation; isochoric deformation tensor; mixed formulation; incompressibility

1 Introduction

Until recently, mechanical characteristics of most of the soft tissue continuum models have been treated as homogeneous where a uniform structure is assumed throughout the computational domain. However, biological tissues often exhibit inhomogeneous mechanical behaviour and therefore exclusion of heterogeneity compromises the accuracy of the predicted results. For example, the mechanical response of a bone is a function of the mineral density which varies spatially (Zannoni et al. 1998). Similarly, in soft tissue organs such as the breast (Riggio et al. 2000) and the face (Mendelson 2009), material heterogeneity exists due to structural variations both at the organ level and locally within each of the tissue types. In addition, when studying the mechanical behaviour of diseased structures, pathologic tissues often display different response to their healthy counterparts (Gupta et al. 1994; Chen

et al. 2008).

Using state-of-the-art imaging techniques, locally varying structural information of biological tissues can often be inferred. However, the challenge in simulating the biomechanics of a heterogeneous body is the modelling complexity. One of the most common methods for handling heterogeneity is through automatic or semi-automatic meshing methods where the geometry of the heterogeneous body is captured using several finite element (FE) meshes. An example is the FE face model in (Barbarino et al. 2009) where a unique mesh is created to describe each individual structure. However, this meshing process is not only time consuming, but can also be computationally expensive due to a large number of degrees of freedom, and the requirement of additional constraints such as tied contact and coupling. Moreover, in many cases, due to the intricacy and microscopic details of heterogeneous structures, it is difficult to replicate the structural variation using this approach.

To simplify the complexity involved in modelling heterogeneous materials, methods have been proposed, in which instead of modifying the mesh geometry, material properties are directly assigned at the numerical integration points (Chen et al. 2010; Mithraratne et al. 2010). However, if a nonlinear, incompressible and hyperelastic constitutive relation is used, this heterogeneous integration points method can become numerically unstable, especially when simulating large deforming bodies. The numerical issue is caused by pseudo residual stresses resulted from the interpolation errors of the pressure field (for incompressible materials) in a mixed FE formulation (Zienkiewicz et al. 2005). In this paper, it is shown that by modifying the constitutive equation using Flory's decomposition of the deformation gradient tensor (Flory 1961), pseudo residual stresses can be eliminated regardless of the interpolatability of the pressure field. Accordingly, using the modified constitutive relations, the integration point based material heterogeneity method can now be applied to nonlinear and incompressible problems for bodies undergoing large deformations. While the method of modifying the constitutive relation for incompressible materials was extensively described by Sussman and Bathe (1987), but to our knowledge, it is the first time that its numerical performance is demonstrated in a heterogeneous setting.

2 Background

Finite elasticity theory is a commonly used approach for describing the mechanics of biological soft tissues, which often undergo large non-linear deformations. A comprehensive

description regarding to the theory of finite elasticity can be found in (Oden 1972). In order to close the system of equations, a constitutive relation that relates the material stress to its strain is required. Although most biological tissues exhibit viscoelastic and sometimes plastic behaviour (Fung 1993), it is a common practice to simplify the materials to be hyperelastic in which only the steady-state elastic deformations are considered. Some examples include the modelling of human facial tissues (Mithraratne et al. 2010), brain tissues (Pezzernenti et al. 2008), breast tissues (Babarenda Gamage, Rajagopal, Nielsen et al. 2011), skeletal muscles (Rohrle et al. 2008) and skin (Hendriks et al. 2003). For hyperelastic materials, the stress-strain relationship can be obtained from a scalar valued strain energy density function w, in which w is the elastic potential energy stored per unit volume due to deformation. The hyperelastic, two-parameter Mooney-Rivlin constitutive relation is used in this study for the purpose of demonstration.

Let $\mathbf{X}$ denotes the position of a material point in the reference configuration, and $\mathbf{x}$ denotes the position of the same material point after some deformation. From this, the deformation gradient tensor $\mathbf{F}$, the Jacobian of transformation J and the Finger deformation tensor $\mathbf{B}$ can be obtained.

$$\begin{aligned} \mathbf{F} &= \partial \mathbf{x} / \partial \mathbf{X} \\ J &= \det \mathbf{F} \\ B &= \mathbf{F}\mathbf{F}^{\mathrm{T}} \end{aligned} \tag{1}$$

The strain energy density function for the Mooney-Rivlin model can be described by a set of strain measures ($I_1 = \mathrm{tr}\mathbf{B}$ and $2I_2 = \mathrm{tr}^2\mathbf{B} - \mathrm{tr}\mathbf{B}^2$) which are invariant under coordinate system transformation.

$$w = c_1(I_1 - 3) + c_2(I_2 - 3) + F_V(J) \tag{2}$$

In equation (2), c_1 and c_2 are the parameters characterising the mechanical stiffness specific to the material, and $F_V(J)$ is the volume regulating term. Since, most biological soft tissues are incompressible due to the high water content (Fung 1993), a Lagrange multiplier function is often introduced to enforce this constraint.

$$F_V(J) = -\lambda(J - 1) \tag{3}$$

The Lagrange multiplier λ is determined to satisfy the incompressibility condition ($J=1$). From the strain energy density function, the Cauchy stress tensor $\boldsymbol{\sigma}$ can be evaluated as

$$\boldsymbol{\sigma} = 2J^{-1}\left(c_1\mathbf{B} + c_2\left(I_1\mathbf{B} - \mathbf{B}^2\right)\right) - \lambda\mathbf{I} \tag{4}$$

where $\mathbf{I}$ is the identity tensor. For incompressible materials, $\boldsymbol{\sigma}$ can be further simplified to

$$\boldsymbol{\sigma} = 2\left(c_1\mathbf{B} + c_2\left(I_1\mathbf{B} - \mathbf{B}^2\right)\right) - \lambda\mathbf{I} \tag{5}$$

Hence equation (5) defines the stress-strain relationship derived from the two-parameter Mooney-Rivlin constitutive relation for incompressible materials. Note that the Lagrange multiplier λ can be seen as a pressure term created to satisfy the incompressibility condition (Oden 1972). This direct method of enforcing incompressibility (without modification to the original strain energy density function) has been widely used for simulating homogeneous structures (see e.g. Whiteley et al. 2007, Rohrle et al. 2008, Flynn et al. 2011).

3 Finite element modelling with material heterogeneity

In finite elasticity with mixed-FEM implementation (Zienkiewicz et al. 2005), the displacement and pressure fields are approximated as piecewise polynomials. In order to satisfy the physical conditions for realistic deformations such as bending and torsion, we use derivative continuous cubic-Hermite basis functions to interpolate the displacement field (Bradley et al. 1997). Moreover, linear-Lagrange basis functions are chosen to interpolate the Lagrange multiplier (pressure) field so that the inf-sup condition for the mixed-FEM formulation is satisfied (Bathe 2001).

In most biomechanical simulations, it is often assumed that deformation is measured from an unstrained reference configuration ($\mathbf{B}_0 = \mathbf{I}$) where the material is also free of external forces. If we substitute $\mathbf{B} = \mathbf{I}$ into equation (5), we arrive at: $\sigma_0 = 2\left(c_1 + 2c_2\right) - \lambda_0$, where λ_0 is the linearly interpolated reference pressure, and σ_0 is a scalar representing the isotropic residual stress ($\boldsymbol{\sigma}_0 = \sigma_0\mathbf{I}$).

In a homogenous problem, c_1 and c_2 are constants throughout the domain; a common practise is to assign an initial value (at the reference configuration) of $\lambda_0 = 2\left(c_1 + 2c_2\right)$ such that the initial residual stresses is set to zero as required for the equilibrium condition. Now consider a heterogeneous problem where the material properties are spatially varying and

arbitrary functions of ξ ($c_1 = c_1(\xi)$ and $c_2 = c_2(\xi)$). Since λ is interpolated from polynomial functions of a fixed order, it is clear that residual stresses cannot, in general, be mathematically set to zero, resulting in a pseudo residual stress.

The reason that λ_0 is dependent on the material parameters is because their respective kinematic tensors are not mutually orthogonal (Criscione et al. 2000), e.g. $\mathbf{B}:\mathbf{I} \neq 0$ and $\left(I_1\mathbf{B}-\mathbf{B}^2\right):\mathbf{I} \neq 0$, with $\mathbf{B}$ and $\left(I_1\mathbf{B}-\mathbf{B}^2\right)$ being the kinematic tensors related to c_1 and c_2, while $\mathbf{I}$ is the kinematic tensor for λ. Therefore, to resolve this problem, it is necessary to modify the constitutive equation such that this dependency is removed. Once this is addressed, zero residual stress can be achieved independent of the element basis functions throughout the domain.

3.1 Modification of the Mooney-Rivlin constitutive relation

Flory (1961) postulated that any deformation $\mathbf{F}$ can be broken into an isochoric (constant volume) distortion component $\overline{\mathbf{F}}$ and a dilatational (volume changing) component $J^{1/3}\mathbf{I}$, such that $\mathbf{F} = J^{1/3}\overline{\mathbf{F}}$ and $\det\overline{\mathbf{F}} = 1$. Based on the isochoric deformation gradient tensor $\overline{\mathbf{F}}$, a new set of invariants can be determined for isochoric strains.

$$\begin{aligned}\bar{I}_1(\mathbf{F}) &= I_1\left(\overline{\mathbf{F}}\right) = J^{-2/3}I_1(\mathbf{F}) \\ \bar{I}_2(\mathbf{F}) &= I_2\left(\overline{\mathbf{F}}\right) = J^{-4/3}I_2(\mathbf{F})\end{aligned} \tag{6}$$

If we redefine the strain energy density function of the Mooney-Rivlin constitutive relation in terms of the isochoric strain invariants, we arrive at the modified Mooney-Rivlin model as shown by Sussman and Bathe (1987).

$$w = \bar{c}_1\left(\bar{I}_1 - 3\right) + \bar{c}_2\left(\bar{I}_2 - 3\right) - \bar{\lambda}(J-1) \tag{7}$$

In equation (7), $\bar{c}_1$ and $\bar{c}_2$ are parameters characterising the mechanical behaviour of isochoric strain, and $\bar{\lambda}$ is a new Lagrange multiplier introduced to enforce material incompressibility in the modified equation. From the modified strain energy density function, the Cauchy stress tensor $\boldsymbol{\sigma}$ can be evaluated as

$$\boldsymbol{\sigma} = 2J^{-1}\left(\bar{c}_1 J^{-2/3}\mathbf{B} + \bar{c}_2 J^{-4/3}\left(I_1\mathbf{B}-\mathbf{B}^2\right) - \left(\frac{1}{3}\bar{c}_1\bar{I}_1 + \frac{2}{3}\bar{c}_2\bar{I}_2\right)\mathbf{I}\right) - \bar{\lambda}\mathbf{I} \tag{8}$$

and setting $J=1$ explicitly for incompressible materials, $\boldsymbol{\sigma}$ becomes

$$\boldsymbol{\sigma}=2\left(\bar{c}_1\mathbf{B}+\bar{c}_2\left(I_1\mathbf{B}-\mathbf{B}^2\right)-\left(\frac{1}{3}\bar{c}_1\bar{I}_1+\frac{2}{3}\bar{c}_2\bar{I}_2\right)\mathbf{I}\right)-\bar{\lambda}\mathbf{I} \tag{9}$$

It can be shown that, the term within the bracket is the stress deviator tensor $\boldsymbol{\sigma}_{\text{dev}}$, whereas $\bar{\lambda}$ is equivalent to the mean normal pressure p, defined as: $p=-\text{tr}\boldsymbol{\sigma}/3$ (see appendix for proof). Consider again, the unstrained reference configuration by substituting $\mathbf{B}=\mathbf{I}$ into equation (9), we arrive at $\sigma_0=-\bar{\lambda}_0$, where zero residual stresses are automatically satisfied when $\bar{\lambda}_0=0$, regardless of the choice of element basis functions.

In the modified Mooney-Rivlin strain energy density function (equation (7)), a new pair of material parameters ($\bar{c}_1, \bar{c}_2$) has to be determined. However, for incompressible materials, $I_1=\bar{I}_1$ and $I_2=\bar{I}_2$, hence, it is clear that with the same material parameters ($c_1=\bar{c}_1$ and $c_2=\bar{c}_2$), the two strain energy density functions are in fact identical.

3.2 Numerical validation

In order to validate the modified constitutive model, the closed-form beam flexure problem proposed by Rivlin (1949) was reproduced in the FE setting. Table 1 shows the values used to obtain the flexure deformation. To ensure that numerical solutions converge to the analytical geometry, a convergence study was conducted (Figure 1). Euclidean errors were calculated from a regular grid of 100 points sampled within the beam. It is important to note that not only did the modified constitutive equation reproduce the analytical solutions accurately, it in fact perform better than the original equation (approximately one order of magnitude more accurate at each refinement step). Figure 2 depicts the simulation results using the most refined mesh consisting of 512 tricubic Hermite elements and 891 nodes.

Published in Computer Methods in Biomechanics and Biomedical Engineering, 18(5): pp. 477-484. DOI: 10.1080/10255842.2013.818662

Table 1. Parameters used for flexure deformation, see (Rivlin 1949) for detail descriptions of the parameters.

Parameter	Value
Reference beam dimensions	$1\times1\times4mm^3$
Mooney-Rivlin constant c_1	1.0kPa
Mooney-Rivlin constant c_2	0.5kPa
Inner flexing radius, r_1	2.0mm
Outer flexing radius, r_2	1.0mm

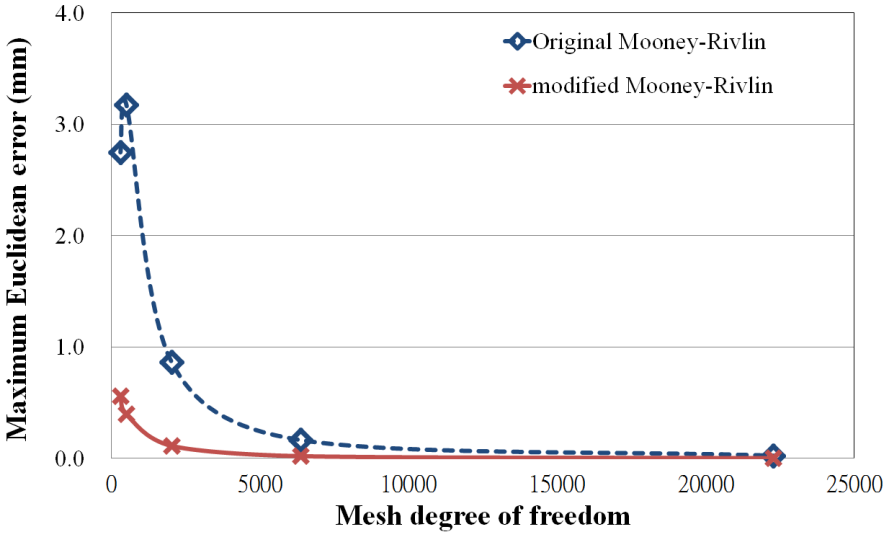

Figure 1. Maximum Euclidean errors convergence with successive mesh refinements for the simulation of beam flexure.

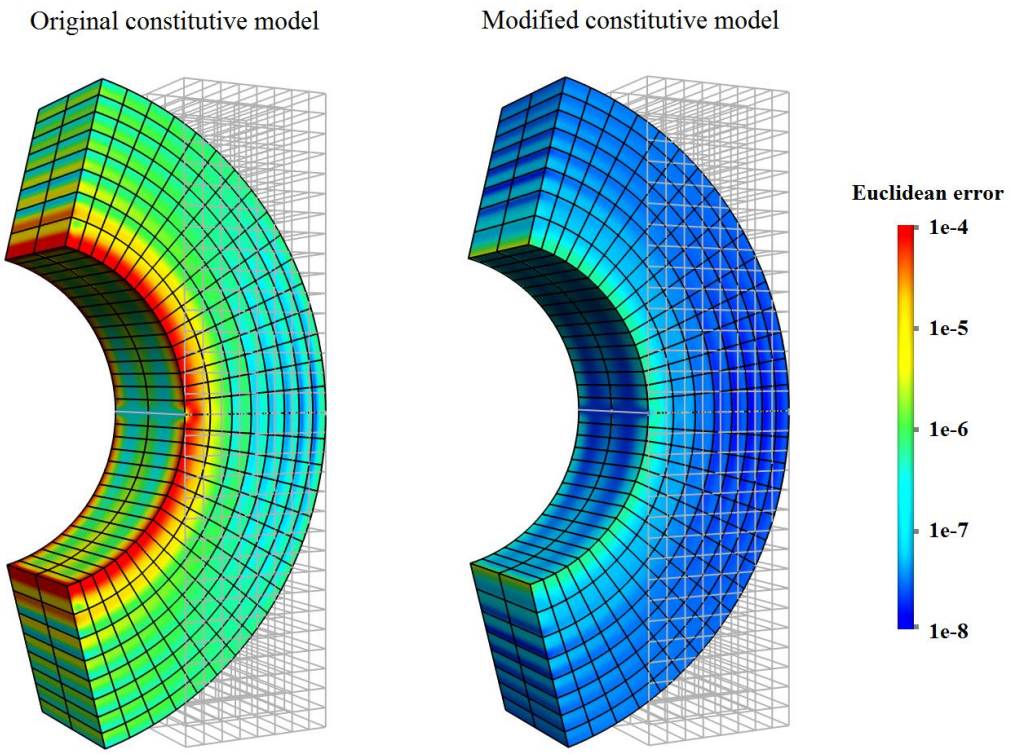

Figure 2. Finite element simulation of flexure deformation using the original and modified Mooney-Rivlin constitutive models. The Euclidean errors are calculated from analytic displacements.

In addition to the flexure deformation, analytic solutions of tensile, compressive and simple shear deformations (Rivlin 1948) on a cube were also simulated. Since the material displacements in these fundamental deformations are linear and homogeneous, converged results were reproduced from a single-element mesh with average Euclidean errors of less than 1×10^{-8}mm, which was the tolerance threshold for the numerical solver. Therefore, it is clear that identical solutions can be obtained using the modified constitutive equation.

4 Simulating heterogeneous materials

4.1 Simulating material interface

Consider an ideal two-material heterogeneous body in which there is a distinct border that separates the materials. When the system is in equilibrium, the normal and shear stresses

acting on the interface, for material points on either side of the boundary, must be equal. If we further assume the materials are kinematically coupled (i.e. displacements in-plane at the interface is bonded), then the physical boundary conditions across this interface can be established as given in table 2 (Zienkiewicz and Gerstner 1960). The normal stress acting on a plane orthogonal to the interface and the normal and shear strains on the interface are discontinuous across the boundary due to the heterogeneity condition, where each material region is required to satisfy a unique and different stress-strain equation.

Table 2. Physical interface condition across material boundaries

	Acting on the interface	**Acting on an orthogonal plane**
Normal stresses	continuous	discontinuous
Normal strains	discontinuous	continuous
Shear stresses	continuous	
Shear strains	discontinuous	

Conventionally, these physical conditions are imposed through contact constraints (e.g. tied contact) between the two materials. However, this approach requires large computational resources for constraint calculations. In addition, biological structures are often complex, with transitions from one tissue type to another occurring at the microscopic level. Therefore, it can be difficult to generate meshes that represent the anatomical geometry.

Alternatively, if the two-material body is assumed to be a single continuum with heterogeneous properties defined at the integration points, then a separated mesh for each material is not required. However, the integration points approach is not an exact representation of the physical conditions described in table 2. Specifically, the FEM explicitly ensures strain continuity through the interpolation of basis functions (intra-element continuity in the case of C0-continuos basis functions and both intra- and inter-element continuity in the case of C1-continuos basis functions). In addition, when Gaussian quadrature scheme is used to evaluate the integrals, it is further anticipated that the internal work, which we are integrating for mechanical analysis, is a continuous polynomial field. As a result, internal stresses and material properties are also continuous.

In order to assess the discrepancies associated with the assumption of a single continuum as opposed to the ideal two-body interfacing condition, an example was set up where a cube of stiff material (c_1 =10kPa and c_2 =5kPa) is coupled to a cube of compliant material (c_1 =1kPa and c_2 =0.5kPa). Two types of material variations within the material were examined; firstly, the material property was described as piecewise linearly varying field (referred to as the linear field method); and secondly, the material property was directly assigned at the integration points allowing more abrupt change to be depicted (referred to as the step change method). Figure 3 illustrates the tensile and compressive deformation of the example problem using the two single continuum methods described above and the tied coupling method (two bodies). In the two body scenario, a distinct discontinuity in the resulting strain was observed. While the sharp discontinuities were smoothed out in both single body cases, the strain profiles were more accurately represented in the step change method where a more abrupt change of the material variation can be captured under the same order of element discretisation.

Moreover, in both cases, the difference in strain was only local to the interface region, and it decreases rapidly further away from the material boundary. Hence, both approaches can be used to approximate the ideal interfacing condition, with the step change method providing a more accurate approximation at the interface region.

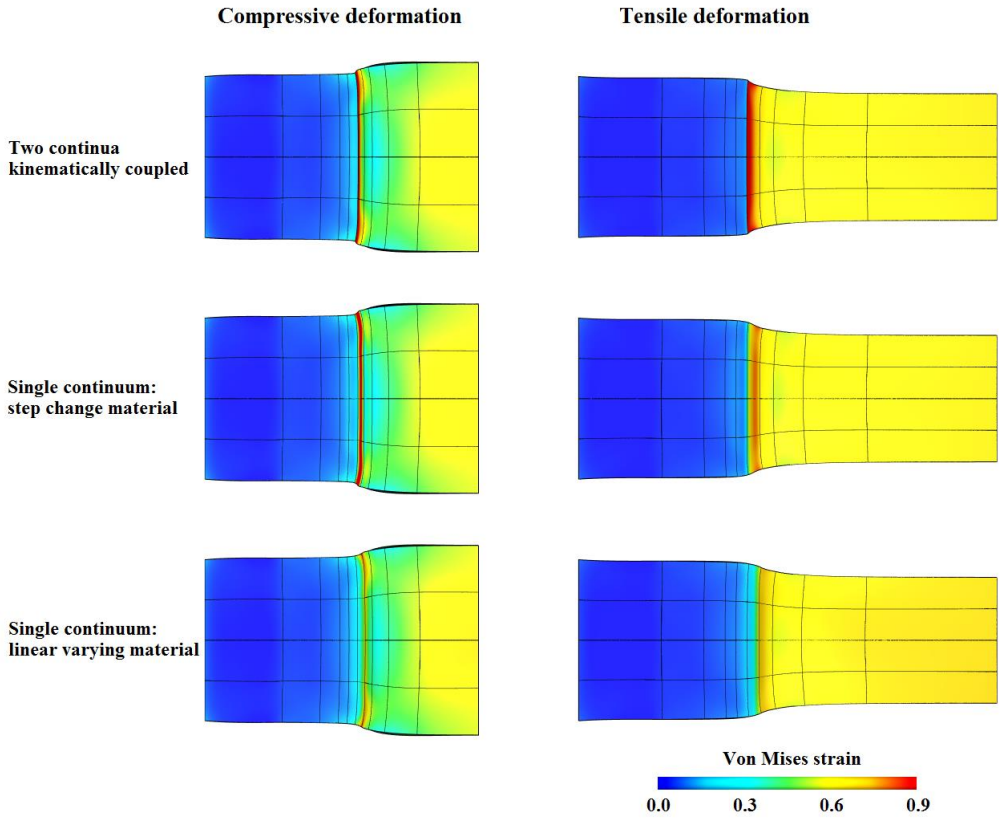

Figure 3. Simulation of compressive and tensile deformations of an ideal two-material-interfacing problem, by applying tied contact between two materials (top), and by assigning heterogeneous material parameters at the integrations points as a step function (centre) and as a piecewise linear field (bottom).

4.2 Application to biomechanical problem

4.2.1 Muscle-tendon complex

Biomechanics of musculoskeletal system is an active area of research in the field of sport science and orthopaedics. In biomechanical analyses of the musculoskeletal system, muscle-tendon units are modelled as one-dimensional linear elements, see e.g. (Li et al. 2002; Cheung and Zhang 2008). This is mostly due to the structural complexity of the muscle-tendon complex. In addition, tendons are on average more than 10000 times tougher than skeletal muscles, hence differences in mechanical stiffness can destabilise a poorly set up nonlinear FE problem. However, having a three-dimensional model of the muscle-tendon complex which undergoes large deformations is a useful tool as the precise location of the maximum stress can provide valuable information for studying muscle damage and fatigue

(Tsui et al. 2004).

The step change method for describing material heterogeneity can be a robust and efficient approach to model the muscle-tendon complex. Figure 4 shows a muscle-tendon complex that has undergone uniaxial stretching. The integration points of tendinous tissue were assigned the material parameters of c_1 =43.3MPa (43300kPa) and c_2 =0, while the integration points of muscular tissue had the material parameters of c_1 =2.5kPa and c_2 =1.175kPa. The Mooney-Rivlin parameters for skeletal muscles were adapted from (Nazari et al. 2010) and the parameters for tendons were estimated relative to the muscle stiffness.

The surface strain field in figure 4 indicates little deformation of the tendinous region due to its much stiffer material properties. Large strain concentrations can be seen at the muscular regions in proximity to the tendons. When under excessive stretch, the blood vessel and other structures in high strain region risk being ruptured or damaged.

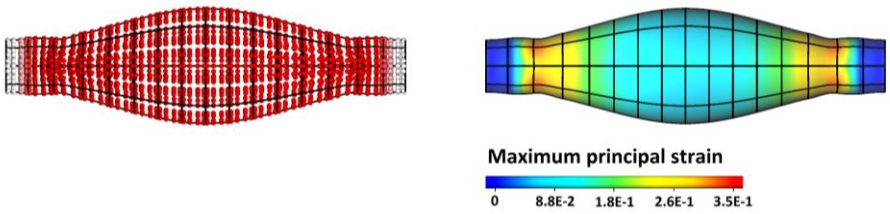

Figure 4. Simulation of the muscle-tendon complex. The spheres on the left represent the material integration points, with white spheres showing the region of tendinous tissue.

4.2.2 Pathologic muscle

The stiffness of skeletal muscle comes primarily from its titin isoforms and the extracellular matrix (Wang et al. 1991; Prado et al. 2005). In pathologic muscles, the structural changes in either titin or the extracellular matrix can significantly reduce their mechanical stiffness (Chen et al. 2008). Modelling the deformation of pathologic muscles can be useful in designing rehabilitation programmes.

A pathologic skeletal muscle model was created in which a portion of the tissue is assumed to be damaged. In our simulations, damaged tissues were assigned material parameters of c_1 =0.75kPa and c_2 =0.352kPa, representing a 70% reduction in the tissue stiffness form the healthy muscles (c_1 =2.5kPa and c_2 =1.175kPa). Figure 5 shows the difference between the mechanical response of healthy and pathologic muscles. It can be seen that the pathologic muscles experience non-uniform deformations that lead to localised strain concentration at the interface between pathologic and healthy tissues. This occurrence is expected as the pathologic region undergoes larger strain due to lower mechanical stiffness.

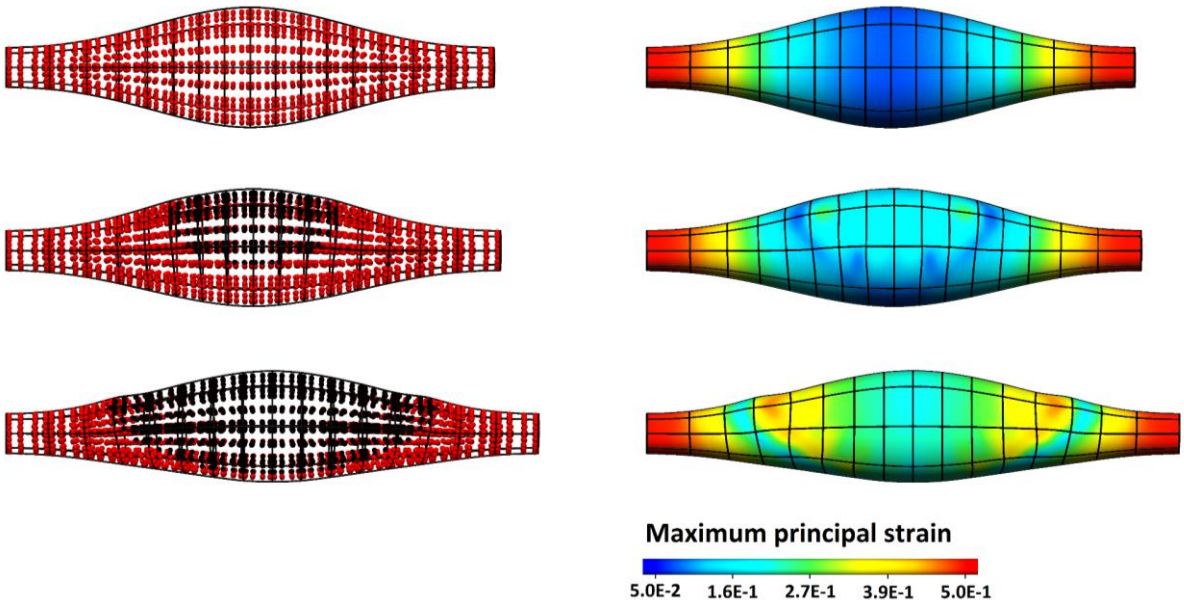

Figure 5. Simulation of healthy muscle (top) and muscles with increasing area of damaged tissues (centre, bottom). The spheres on the left represent the material integration points, with black spheres showing the pathologic region.

5 Conclusion and discussion

When using the mixed (displacement-pressure) FE formulation to study the mechanical behaviour of an incompressible and heterogeneous body, it was shown that the presence of pseudo residual stresses compromise the stability of the solution. However, these residual stresses can be removed by modifying the constitutive relation using the isochoric deformation gradient tensor. In addition, this study demonstrated that the modified

constitutive relation leads to an improved numerical performance for homogeneous materials (flexure of a homogeneous beam).

The most important difference between the modified and the original constitutive equations is the representation of the pressure field (λ and $\bar{\lambda}$). In the modified equation, the mean normal pressure is evaluated directly as an independent field ($\bar{\lambda} = p$). Whereas in the original equation, pressure is related to the material parameters and the strain invariants (i.e. $\lambda = p + (2c_1 I_1 + 4c_2 I_2)/3$). Accordingly, the numerical properties of these two equations are fundamentally different. We believe the improvement observed when using the modified constitutive equation, is due to $\bar{\lambda}$ field being more linear than λ, therefore, when approximating it with the same polynomial order, using linear-Lagrange basis functions, $\bar{\lambda}$ can be represented more accurately. The nonlinearity of λ field is possibly due to its dependence on I_1 and I_2, which are derived from the cubic-Hermite interpolated displacement field. As a result, the variation of I_1 and I_2 which constitutes λ cannot be represented as accurately when using linear basis functions.

This study also demonstrated that when modelling a heterogeneous continuum with distinct material boundary, it is more appropriate to assign material properties directly at the integration points of the FE mesh, rather than interpolating them from a polynomial field (e.g. linear). This is because interpolation of the material field results in a loss of accuracy, whereas assigning the values directly at the point of interest retains the step change characteristic of the material. By assigning material properties at the integration points, together with the modified constitutive relation, two musculoskeletal problems were examined. In both cases, converged results were obtained with a relatively coarse FE mesh. Furthermore, since the modification strategy described here operates on the deformation gradient tensor, it can be intuitively extended to other hyperelastic constitutive relations for modelling more complex material behaviours.

In practice, the structural information of heterogeneous biological tissues can be determined at the integration points from imaging modalities such as computed tomography (for bone and cartilage), and magnetic resonance imaging or ultrasound imaging (for soft tissue structures). This structural information in combination with mechanical testing procedures for identifying tissue properties enables modellers to create complex, subject-specific biomechanical models. Examples of mechanical tests include *in vivo* surface indentation (Tran et al. 2007; Flynn et al. 2011), suction (Barbarino et al. 2011; Hendriks et al.

2006), uniaxial extension (Lim et al. 2008) and experiments involving gravitational loading (Babarenda Gamage, Rajagopal, Ehrgott et al. 2011).

Acknowledgement

The work presented in this paper was funded by Foundation for Research, Science and Technology of New Zealand under the grant number UOAX0712. The authors would like to thank the anonymous reviewers for their invaluable comments and suggestions. Moreover, the authors would also like to acknowledge Mr. Thiranja Babarenda Gamage, Professor Martyn Nash and Professor Poul Nielsen at the Auckland Bioengineering Institute for their thoughtful input into the discussion regarding to the material interfaces.

Appendix

This appendix reviews the proof that $\bar{\lambda}$ in equation (9) is equivalent to the mean normal pressure of the Cauchy stress. We begin by setting the first terms in the equation (9) as $\bar{\boldsymbol{\sigma}}$:

$$\boldsymbol{\sigma} = \bar{\boldsymbol{\sigma}} - \bar{\lambda}\mathbf{I} \text{ with } \bar{\boldsymbol{\sigma}} = 2\left(\bar{c}_1\mathbf{B} + \bar{c}_2\left(I_1\mathbf{B} - \mathbf{B}^2\right) - \left(\frac{1}{3}\bar{c}_1\bar{I}_1 + \frac{2}{3}\bar{c}_2\bar{I}_2\right)\mathbf{I}\right)$$

By definition, the Cauchy stress tensor can be expressed as a sum of the stress deviator tenor $\boldsymbol{\sigma}_{\text{dev}}$ and the volumetric stress tensor ($\sigma\mathbf{I}$), where σ is mean normal stress ($\sigma = \text{tr}\boldsymbol{\sigma}/3$):

$$\boldsymbol{\sigma} = \boldsymbol{\sigma}_{\text{dev}} + \sigma\mathbf{I} = \bar{\boldsymbol{\sigma}} - \bar{\lambda}\mathbf{I}$$

Taking the trace of this equation (Note that $\text{tr}\bar{\boldsymbol{\sigma}} = 0$ according to our designation of $\bar{\boldsymbol{\sigma}}$ and $\text{tr}\boldsymbol{\sigma}_{\text{dev}} = 0$ by definition), we arrive at: $\bar{\lambda} = -\sigma = p$, where p is the mean normal pressure of the Cauchy stress tensor ($p = -\text{tr}\boldsymbol{\sigma}/3$). And from this, $\bar{\boldsymbol{\sigma}} = \boldsymbol{\sigma} + p\mathbf{I} = \boldsymbol{\sigma}_{\text{dev}}$ is the stress deviator tenor.

Reference

Babarenda Gamage TP, Rajagopal V, Ehrgott M, Nash MP, Nielsen PMF. 2011. Identification of mechanical properties of heterogeneous soft bodies using gravity loading. Int J Numer Meth Bio. 27(4):391-407.

Babarenda Gamage TP, Rajagopal V, Nielsen PMF, Nash MP. 2011. Patient-specific modeling of breast biomechanics with applications to breast cancer detection and

treatment. In: Studies in Mechanobiology, Tissue Engineering and Biomaterials. Heidelberg ; New York (NY): Springer. p. 1-34.

Barbarino GG, Jabareen M, Mazza E. 2011. Experimental and numerical study on the mechanical behavior of the superficial layers of the face. Skin Res Technol. 17(4):434-444.

Barbarino GG, Jabareen M, Trzewik J, Nkengne A, Stamatas G, Mazza E. 2009. Development and validation of a three-dimensional finite element model of the face. J Biomech Eng. 131(4):041006.

Bathe KJ. 2001. The inf–sup condition and its evaluation for mixed finite element methods. Comput Struct. 79(2):243-252.

Bradley CP, Pullan AJ, Hunter PJ. 1997. Geometric modeling of the human torso using cubic hermite elements. Ann Biomed Eng. 25(1):96-111.

Chen G, Schmutz B, Epari D, Rathnayaka K, Ibrahim S, Schuetz MA, Pearcy MJ. 2010. A new approach for assigning bone material properties from CT images into finite element models. J Biomech. 43(5):1011-1015.

Chen Q, Manduca A, An K-N. 2008. Characterization of skeletal muscle elasticity using magnetic resonance elastography. US Musculoskeletal Review. 3(1):60-63.

Cheung JTM, Zhang M. 2008. Parametric design of pressure-relieving foot orthosis using statistics-based finite element method. Med Eng Phys. 30(3):269-277.

Criscione JC, Humphrey JD, Douglas AS, Hunter WC. 2000. An invariant basis for natural strain which yeilds orthogonal stress response terms in isotropic hyperelasticity. J Mech Phys Solids. 48(12):2445-2465

Flory PJ. 1961. Thermodynamic relations for high elastic materials. T Faraday Soc. 57:829-838.

Flynn C, Taberner A, Nielsen P. 2011. Modeling the mechanical response of in vivo human skin under a rich set of deformations. Ann Biomed Eng. 39(7):1935-1946

Fung YC. 1993. Biomechanics : mechanical properties of living tissues. 2nd ed. New York (NY): Springer-Verlag.

Gupta KB, Ratcliffe MB, Fallert MA, Edmunds Jr LH, Bogen DK. 1994. Changes in passive mechanical stiffness of myocardial tissue with aneurysm formation. Circulation. 89(5):2315-2326.

Hendriks FM, Brokken D, Oomens CWJ, Bader DL, Baaijens FPT. 2006. The relative contributions of different skin layers to the mechanical behavior of human skin in vivo using suction experiments. Med Eng Phys. 28(3):259-266.

Hendriks FM, Brokken D, van Eemeren JT, Oomens CW, Baaijens FP, Horsten JB. 2003. A numerical-experimental method to characterize the non-linear mechanical behaviour of human skin. Skin Res Technol. 9(3):274-283.

Li G, Suggs J, Gill T. 2002. The effect of anterior cruciate ligament injury on knee joint function under a simulated muscle load: a three-dimensional computational simulation. Ann Biomed Eng. 30(5):713-720.

Lim KH, Chew CM, Chen PC, Jeyapalina S, Ho HN, Rappel JK, Lim BH. 2008. New extensometer to measure in vivo uniaxial mechanical properties of human skin. J Biomech. 41(5):931-936.

Mendelson B. 2009. Facelift anatomy, SMAS, retaining ligaments and facial spaces. In: Aesthet Plast Surg. Edinburgh: Saunders. p. 6:1-22.

Mithraratne K, Hung A, M.Sagar, Hunter PJ. 2010. An efficient heterogeneous continuum model to simulate active contraction of facial soft tissue structures. In: 6th World Congress of Biomechanics (WCB 2010); August 1-6, 2010; Singapore. Berlin ; Heidelberg: Springer. p. 1024-1027.

Nazari MA, Perrier P, Chabanas M, Payan Y. 2010. Simulation of dynamic orofacial movements using a constitutive law varying with muscle activation. Comput Methods Biomech Biomed Engin. 13(4):469-482.

Oden JT. 1972. Finite elements of nonlinear continua. New York (NY): McGraw-Hill.

Pezzernenti Z, Ursu D, Misra S, Okamura AM. 2008. Modeling realistic tool-tissue interactions with haptic feedback: a learning-based method. Symposium on Haptics Interfaces for Virtual Environment and Teleoperator Systems 2008, Proceedings.209-215.

Prado LG, Makarenko I, Andresen C, Kruger M, Opitz CA, Linke WA. 2005. Isoform diversity of giant proteins in relation to passive and active contractile properties of rabbit skeletal muscles. J Gen Physiol. 126(5):461-480.

Riggio E, Quattrone P, Nava M. 2000. Anatomical study of the breast superficial fascial system: the inframammary fold unit. Eur J Plast Surg. 23(6):310-315.

Rivlin RS. 1948. Large elastic deformations of isotropic materials. IV. further developments of the general theory. Philos Trans R Soc Lond A. 241(835):379-397.

Rivlin RS. 1949. Large elastic deformations of isotropic materials. V. the problem of flexure. Proc R Soc Lond A Math Phys Sci. 195(1043):463-473.

Rohrle O, Davidson JB, Pullan AJ. 2008. Bridging Scales: A three-dimensional electromechanical finite element model of skeletal muscle. SIAM J Sci Comput. 30(6):2882-2904.

Sussman T, Bathe KJ. 1987. A finite-element formulation for nonlinear incompressible elastic and inelastic analysis. Comput Struct. 26(1-2):357-409.

Tran HV, Charleux F, Rachik M, Ehrlacher A, Ho Ba Tho MC. 2007. In vivo characterization of the mechanical properties of human skin derived from MRI and indentation techniques. Comput Methods Biomech Biomed Engin. 10(6):401-407.

Tsui CP, Tang CY, Leung CP, Cheng KW, Ng YF, Chow DHK, Li CK. 2004. Active finite element analysis of skeletal muscle-tendon complex during isometric, shortening and lengthening contraction. Biomed Mater Eng. 14(3):271-279.

Wang K, McCarter R, Wright J, Beverly J, Ramirez-Mitchell R. 1991. Regulation of skeletal muscle stiffness and elasticity by titin isoforms: a test of the segmental extension model of resting tension. Proc Natl Acad Sci U S A. 88(16):7101-7105.

Whiteley JP, Gavaghan DJ, Chapman SJ, Brady JM. 2007. Non-linear modelling of breast tissue. Math Med Biol. 24(3):327-345

Zannoni C, Mantovani R, Viceconti M. 1998. Material properties assignment to finite element models of bone structures: a new method. Med Eng Phys. 20(10):735-740.

Zienkiewicz OC, Gerstner RW. 1960. A stress-function approach to interface and mixed boundary-condition problems (boundary conditions and finite-difference techniques). Int J Mech Sci. 2(1-2): 93-101.

Zienkiewicz OC, Taylor RL, Zhu JZ. 2005. The finite element method : its basis and fundamentals. 6th ed. Amsterdam ; London: Elsevier Butterworth-Heinemann.